Defence Technology 13 (2017) 22–32

Contents lists available at ScienceDirect

Defence Technology

journal homepage: www.elsevier.com/locate/dt

Thermal decomposition and kinetics of plastic bonded explosives based on mixture of HMX and TATB with polymer matrices

Arjun Singh [a, b, *], Tirupati C. Sharma [a], Mahesh Kumar [a], Jaspreet Kaur Narang [a], Prateek Kishore [a], Alok Srivastava [b]

[a] Terminal Ballistics Research Laboratory, Defence Research & Development Organisation, Ministry of Defence, Explosive Division, Sector 30, Chandigarh (UT), 160030, India
[b] Department of Chemistry & Centre for Advanced Studies in Chemistry, Panjab University, Chandigarh, 160 014, India

ARTICLE INFO

Article history:
Received 21 August 2016
Received in revised form
13 November 2016
Accepted 28 November 2016
Available online 23 December 2016

Keywords:
Plastic bonded explosives
Thermogravimetric analysis
Differential scanning calorimeter
Thermal decomposition
Kinetics

ABSTRACT

This work describes thermal decomposition behaviour of plastic bonded explosives (PBXs) based on mixture of l,3,5,7-tetranitro- 1,3,5,7-tetrazocane (HMX) and 2,4,6- triamino-1,3,5-trinitrobenzene (TATB) with Viton A as polymer binder. Thermal decomposition of PBXs was undertaken by applying simultaneous thermal analysis (STA) and differential scanning calorimetry (DSC) to investigate influence of the HMX amount on thermal behavior and its kinetics. Thermogravimetric analysis (TGA) indicated that the thermal decomposition of PBXs based on mixture of HMX and TATB was occurred in a three-steps. The first step was mainly due to decomposition of HMX. The second step was ascribed due to decomposition of TATB, while the third step was occurred due to decomposition of the polymer matrices. The thermal decomposition % was increased with increasing HMX amount. The kinetics related to thermal decomposition were investigated under non-isothermal for a single heating rate measurement. The variation in the activation energy of PBXs based on mixture of HMX and TATB was observed with varying the HMX amount. The kinetics from the results of TGA data at various heating rates under non-isothermal conditions were also calculated by Flynn–Wall–Ozawa (FWO) and Kissinger-Akahira-Sunose (KAS) methods. The activation energies calculated by employing FWO method were very close to those obtained by KAS method. The mean activation energy calculated by FWO and KAS methods was also a good agreement with the activation energy obtained from single heating rate measurement in the first step decomposition.

1. Introduction

Plastic bonded explosives (PBXs) based on l,3,5,7-tetranitro-1,3,5,7-tetrazocane (HMX) or 2,4,6-triamino-1,3,5- trinitrobenzene (TATB) with various polymer matrices have been formulated in the literature [1–16]. Polymer matrices; Viton A; a vinylidene fluoride - hexafluoropropylene copolymer, Kel-F 800; a vinylidene fluoride - chlorotrifluoroethylene copolymer, polytetrafluoroethylene, Estane 5703; a poly(ester urethane) block copolymer etc. are mainly used for PBXs formulation due to their higher loading density, homogeneity, better dimensional integrity and higher thermal stability than TNT based melt cast compositions. The role of polymeric matrices is to minimise their sensitivity, improved mechanical and high thermal properties [17].

TATB based PBXs formulations such as LX-17 and PBX 9502 [18–21] have been developed for nuclear bomb, missiles and space applications. TATB has a high thermal stability, insensitive in terms of impact and friction but poor performance. The performance of formulations has been enhanced either to use new explosive molecule having better performance than TATB or admixture of high energetic materials which has a high performance and comparatively less sensitive to ensure the safety parameters [22–24]. Therefore, PBXs based on HMX and TATB have been formulated with polymer matrices; Estane, Viton A and Kel-F 800 to some extent compromise with insensitivity [25,26]. These formulations have been characterized in terms of density, detonation velocity, ignition temperature and other explosive properties which

* Corresponding author. Terminal Ballistics Research Laboratory, Defence Research & Development Organisation, Ministry of Defence, Explosive Division, Sector 30, Chandigarh (UT), 160030, India.
E-mail address: arjunsngh@yahoo.com (A. Singh).
Peer review under responsibility of China Ordnance Society.

http://dx.doi.org/10.1016/j.dt.2016.11.005

are covered under few reports and in paper also [27–37]. The thermal decomposition behaviour and kinetics are very important because it ensures safety parameters during handling, processing, production and storage [38–40]. PBXs based on HMX or TATB have been extensively investigated for the thermal decomposition behaviour and its kinetics [41–44] by means of non-isothermal thermogravimetry (TGA) and differential scanning calorimetry (DSC). The kinetic parameters of HMX based PBXs with Viton A [45], C4 [46], Formex [47] and Semtex [48,49] have been investigated and published. Brunham and Weese [50] have investigated the kinetics of PBXs with three endothermic binders; Estane 5703, Viton A and Kel-F 800 by performing TG measurements at different heating rates, exhibited that Viton A and Kel-F 800 were more thermally stable than HMX and TATB. Craig et al. [51] have been studied thermal behaviour of PBXs based on HMX or TATB with same endothermic binders, exhibited longer times to thermal explosion than those of pure HMX or TATB in the one-dimensional time to explosion and in other thermal experiments [52,53].

Moreover, the decomposition kinetic models with different polymeric matrices have been published as both kinetic parameters and reaction models are the key factor for the prediction of the thermal hazard properties. It has been reported that the effect of the polymer matrices on the decomposition mechanism has been significantly observed and resulting in very different reaction models. Tarver and Tran have also been measured the decomposition models to predict of explosion and the locations within the explosive charges [54]. However, the thermal decomposition behaviour and kinetics of PBXs based on mixture of TATB and HMX with Viton A are less addressed in an open literature. In our previous study [55], the mechanical and explosive properties of PBXs based on mixture of HMX and TATB have been investigated and published.

In the present work, the thermal decomposition behaviour of PBXs based on mixture of HMX and TATB with Viton A as polymeric matrices is studied by employing Simultaneous Thermal Analysis (STA) and DSC. The kinetic parameters namely the activation energy and pre-exponential factor are determined under non-isothermal conditions for a single heating rate measurement. The three dynamic TGA measurements at different heating rates are also used to investigate activation energy as a function of reaction conversion through non-isothermal condition by employing Flynn–Wall–Ozawa (FWO) and Kissinger-Akahira-Sunose (KAS) methods.

2. Experimental

2.1. Materials

HMX which is prepared in-house by nitration of hexamine by Bechmann reaction was used for PBXs formulation. Other ingredient TATB obtained from High Energy Material Research Laboratory Pune, India was used as received. Viton A; copolymer of vinylidene fluoride and hexafluoropropylene manufactured by 3M DuPont Corporation was served as a polymer binder as received. Methyl ethyl ketone procured from SD Chem. Ltd. Pvt. India was used as received.

2.2. Preparation of PBXs

PBXs formulations were prepared from a mixture of TATB and HMX with Viton A by slurry coating process as described in our previous work [55]. In this process, a mixture of HMX and TATB was dispersed with 3000 ml of a water with continuous stirring at 60 °C. Then, polymer solution prepared in a methyl ethyl ketone was added to the above mixture. The temperature was raised to 90 °C to evaporate the solvent from the solution. Then, the polymer was precipitated on the surface of energetic materials. Finally, filtered and dried to get PBXs. In this way, PBXs from a mixture of HMX and TATB at varying mass ratios (10:80, 20:70, 30:60, 40:50, 50:40, 60:30, 70:20 and 80:10 respectively) with 10 weight percent of Viton A were formulated and designated as HT1080, HT2070, HT3060, HT4050, HT5040, HT6030, HT7020 and HT8010 respectively. For comparison, HMX/Viton A and TATB/Viton A formulations (90:10 by weight percent of HMX or TATB with Viton A) were also formulated.

2.3. Characterization of PBXs

Non-isothermal thermo-gravimetric (TG) analyses of PBXs were carried out by Simultaneous Thermal Analyzer (STA), manufactured and supplied by METTLER TOLEDO, Model Mettler Toledo 851[e]. The samples were subjected to heating from 25 °C to 600 °C at heating rate 10 °C/min under nitrogen atmosphere. HT4050 sample was also subjected to heating from 25 °C to 600 °C at different heating rates 10, 20 and 30 °C/min under nitrogen atmosphere.

DSC analyses were carried out in sealed standard 40 μL aluminum crucible using a Differential Scanning Calorimeter (DSC), manufactured and supplied by METTLER TOLEDO, Model DSC 823[e]. 4.0 ± 0.5 mg weight of the sample was used for each experiment. The samples were scanned from 25 °C to 600 °C for each experiment at heating rate 10 °C/min under nitrogen atmosphere. TG and DSC analyses of pure HMX, TATB and Viton A were also monitored under similar conditions.

3. Results and discussion

3.1. TG/DTG studies

Fig. 1 shows TG thermograms of HMX, TATB, Viton A and PBXs namely HT1080, HT2070, HT3060, HT4050, HT5040, HT6030, HT7020, HT8010, HMX/Viton A and TATB/Viton A. TG thermogram of HMX shows that 99.9% weight loss occurs in a single step as a sharp thermal decomposition strips at 280 °C [18,56]. TG thermogram of TATB shows 87.7% weight loss in a single step over a wide range of the temperature (300 °C –450 °C). The main weight loss occurs within a range of 350 °C –385 °C due to the thermal decomposition of TATB [52]. TG thermogram of Viton A shows that weight loss occurs in a single step at a high temperature within a range of 458 °C –504 °C due to the thermal decomposition of polymer matrices.

TG thermograms of PBXs; HT1080, HT2070, HT3060, HT4050, HT5040, HT6030, HT7020 and HT8010 show that the weight loss occurs in a three steps, but the thermal stability causes a decay of a first one. The weight loss occurs in the first step at 278 °C–287 °C due to thermal decomposition of HMX; while weight loss occurs in a second step in a range of 307 °C–374 °C due to the thermal decomposition TATB. The weight loss occurs in a third step in a range of 456 °C–498 °C due to thermal decomposition of polymer matrices. HMX/Viton A and TATB/Viton A samples also show two steps weight loss; the weight loss in the first step is due to decomposition of the HMX or TATB, whereas weight loss in the second step is due to decomposition of polymer matrices. Thermal decomposition % obtained at different stages during decomposition process from TG thermograms is summarized in Table 1.

As far as thermal stability is concerned, it is reported that small weight loss of a materials at a certain temperature, more is thermally stable. The results indicate that 9–72% weight loss of PBXs based on mixture of HMX and TATB is occurred in the first step due to thermal decomposition of HMX. It is also observed that the decomposition % in the first step is increased with increasing HMX

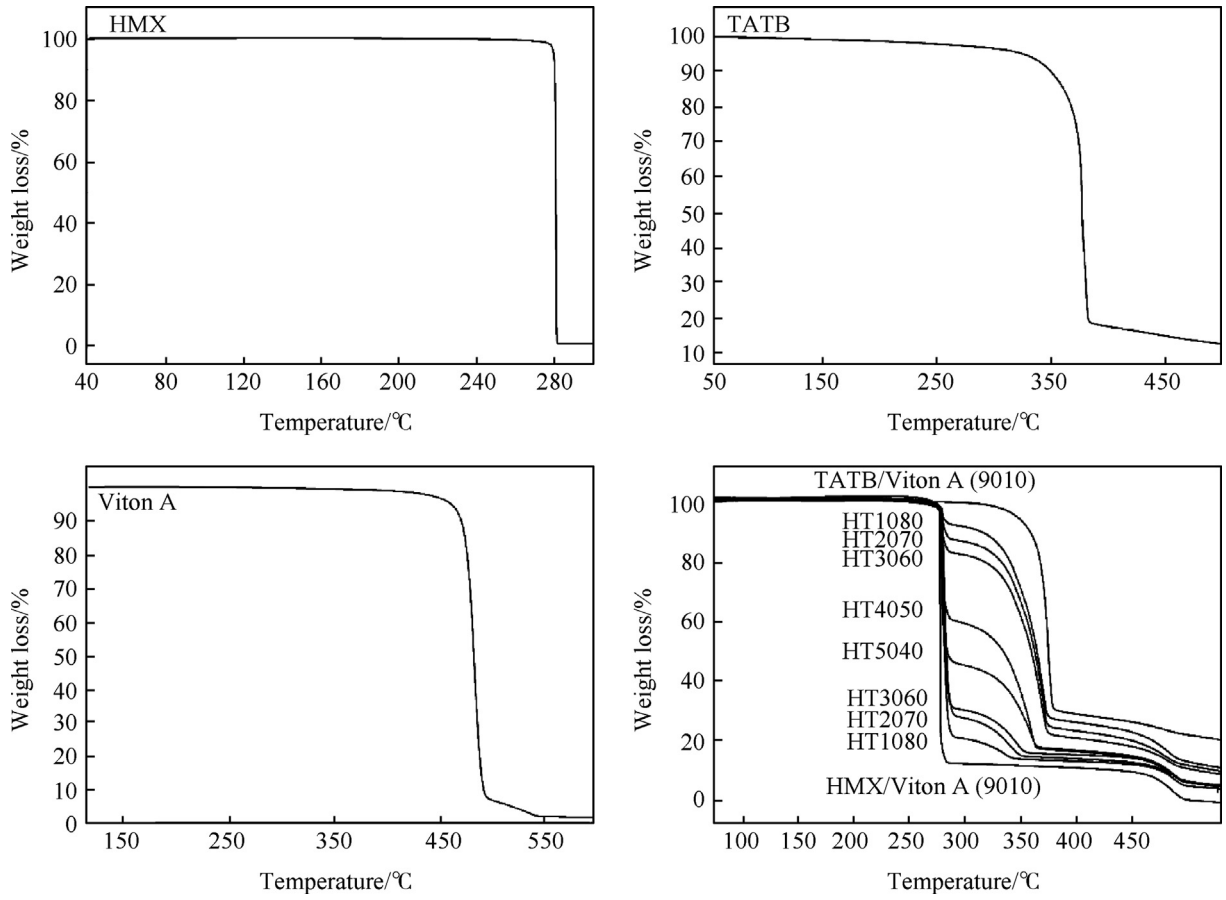

Fig. 1. TG thermograms of HMX, TATB, Viton A and PBXs obtained at heating rate 10 °C/min under nitrogen atmosphere.

Table 1
TG data of PBXs along with HMX, TATB and Viton A obtained from TG thermograms at heating rate 10 °C/min under nitrogen atmosphere.

Sample	Multisteps thermal decomposition			Decomposition
	SDT[a] FDT[b] (270 °C –290 °C) /wt.%	SDT[a] FDT[b] (290 °C –450 °C) /wt.%	SDT[a] FDT[b] (450 °C –550 °C) /wt.%	/%
HT1080	7.5	71.1	12.5	91.1
HT2070	13.4	67.5	11.2	92.2
HT3060	17.5	63.6	11.7	92.8
HT4050	40.4	44.7	11.2	96.4
HT5040	54.1	31.0	11.3	96.5
HT6030	69.9	15.8	10.6	96.6
HT7020	74.9	11.9	10.7	97.4
HT8010	79.1	8.9	8.1	97.8
HMX/Viton A	87.5	1.7	10.1	99.4
TATB/Viton A	0.5	73.2	10.7	83.7
HMX	99.7	–	–	99.9
TATB	1.0	85.8	0.9	87.9
Viton A	–	0.4	97.9	98.6

[a] Starting decomposition temperature.
[b] Final decomposition temperature.

amount. This implies that PBXs are comparatively exhibited to better thermal stability with less HMX amount. The decomposition % in the first step is not exactly found to same as the initial weight of HMX due to a high thermal conductivity of TATB causes the neighbouring HMX molecules to heat up and fast burning more quickly than pure HMX [51]. Other reason for discrepancy in the results may be due to different particle size i.e. coarse HMX and fine TATB crystals [49] used for formulations as well as the small amount of sample used for TG analysis.

Fig. 2 shows that the derivative thermogravimetric (DTG) thermograms of HMX, TATB and Viton A show a single peak of maximum thermal decomposition. The HT1080, HT2070, HT3060, HT4050, HT5040, HT6030, HT7020 and HT8010 show three peaks; the first peak appears due to the thermal decomposition of HMX, the second peak appears due to the thermal decomposition of TATB and the third peak appears due to the thermal decomposition of

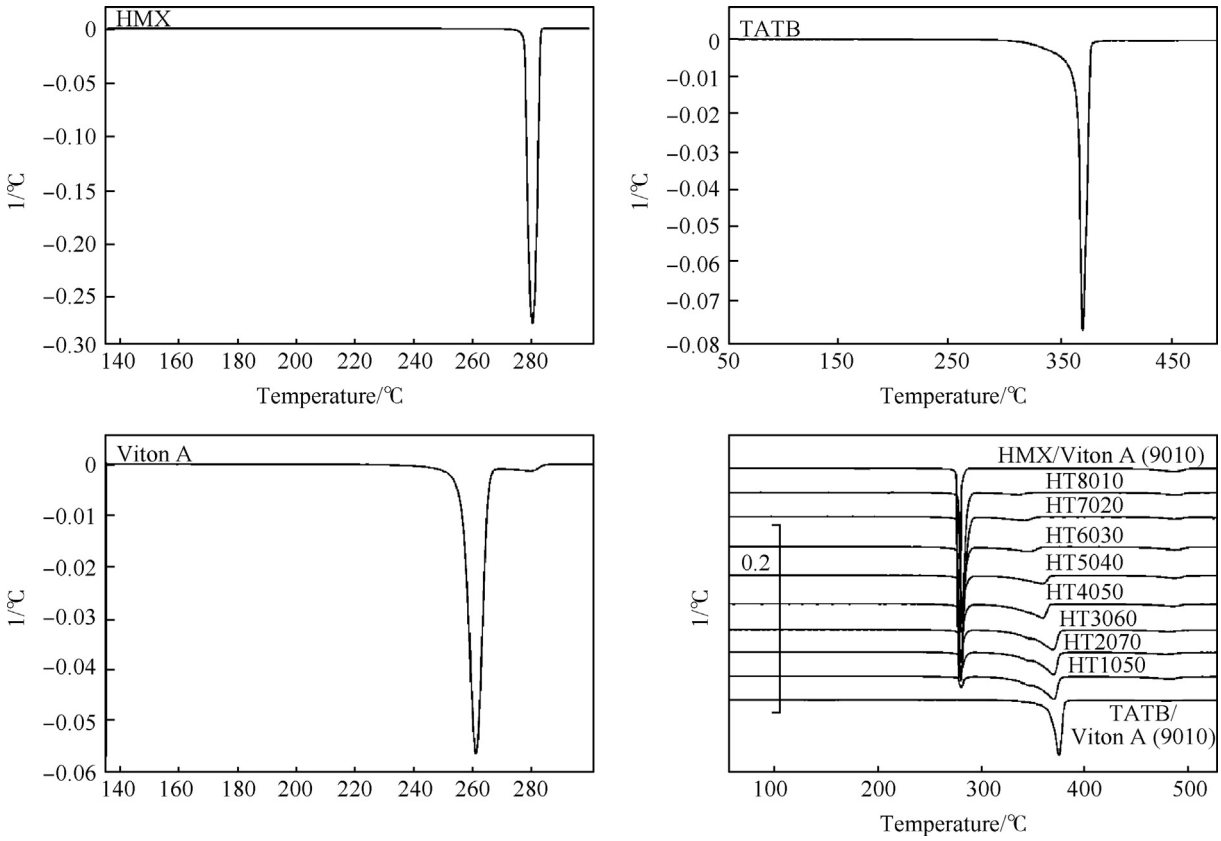

Fig. 2. DTG thermograms of HMX, TATB, Viton A and PBXs obtained at heating rate 10 °C/min under nitrogen atmosphere.

polymer matrices. HMX/Viton A and TATB/Viton A samples show two peaks; the first peak attributes to the thermal decomposition of HMX or TATB, while the second peak ascribes to the thermal decomposition of polymer matrices. DTG thermograms can be easily distinguished as when the thermal decomposition ends and the next decomposition begins. Thermal data in terms of TG onset temperature (T_{onset}), endset temperature (T_{endset}) and peak temperature for maximum thermal decomposition (T_{max}) are listed in Table 2. It is observed that T_{onset} and T_{max} values are slightly increased with increasing HMX amount from 10 to 80 wt. %. The results also suggest that the HMX, TATB and Viton A are compatible with each other.

3.2. DSC studies

DSC curves of HMX, TATB, Viton A and PBXs based on mixture of HMX and TATB are shown in Fig. 3. DSC curve of HMX shows three endo-/exo-thermic peaks in the DSC curve. The first endothermic peak appears at 189 °C due to β to δ-HMX polymorph transformation. The second endothermic peak appears at 278 °C which corresponds to melting point (T_m), followed by the third exothermic peak at 287 °C due to the thermal decomposition of HMX [54,57]. DSC curve of TATB exhibits a single exothermic peak at 388 °C due to the thermal decomposition of TATB. The thermal properties such as glass transition temperature (T_g) and softening

Table 2
Thermal data in terms of T_{onset}, T_{endset} and T_{max} obtained from TG/DTG thermograms of PBXs along with HMX, TATB and Viton A.

Sample	Thermal decomposition								
	T_{onset}	T_{endset}	T_{max}	T_{onset}	T_{endset}	T_{max}	T_{onset}	T_{endset}	T_{max}
	(270 °C –290 °C)			(290 °C –450 °C)			(450 °C –550 °C)		
HT1080	278.1	385.7	280.2	348.4	373.9	369.7	467.3	495.6	482.9
HT2070	278.3	282.4	280.7	346.5	373.6	369.6	470.7	486.9	478.5
HT3060	279.2	281.7	280.7	340.5	363.9	359.4	471.0	495.6	480.3
HT4050	279.7	281.9	280.8	340.2	363.9	358.8	474.2	495.3	481.1
HT5040	279.5	281.4	280.8	337.5	363.7	357.3	473.2	493.7	486.6
HT6030	279.0	283.0	281.3	329.1	353.9	344.4	473.3	495.7	486.8
HT7020	279.4	286.1	281.5	309.1	326.4	335.2	472.3	495.7	487.7
HT8010	279.9	286.0	283.7	321.4	321.4		473.3	497.2	486.8
HMX/Viton A	279.9	286.8	281.0	–	–	–	470.1	497.5	487.4
TATB/Viton A	–	–	–	361.3	393.2	375.5	441.2	480.9	476.2
HMX	282.3	292.6	285.3	–	–	–	–	–	–
TATB	–	–	–	352.7	383.4	376.7	–	–	–
Viton A	–	–	–	–	–	–	458.8	503.5	493.3

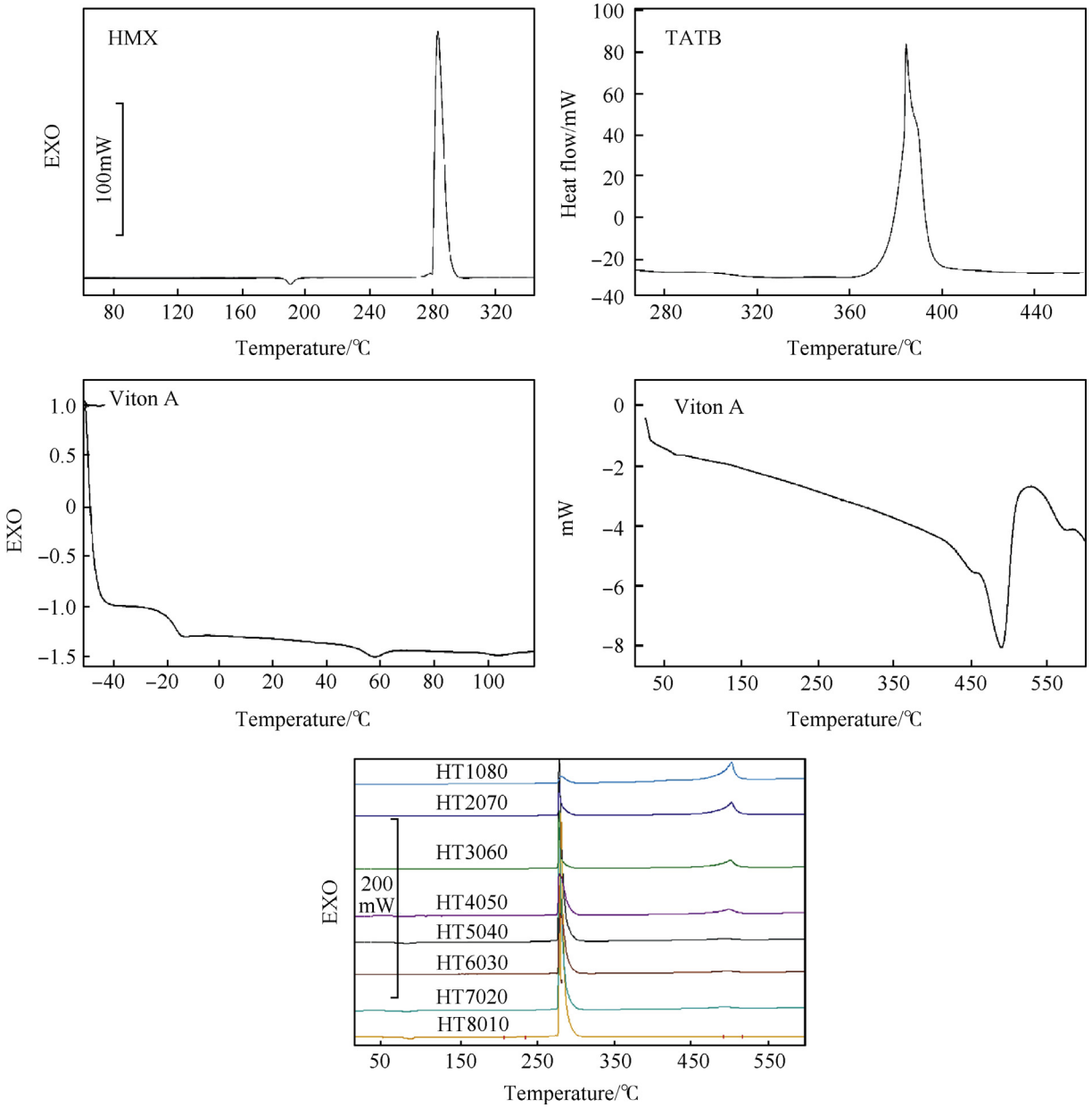

Fig. 3. DSC curves of HMX, TATB, Viton A and PBXs samples at heating rate 10 °C/min under nitrogen atmosphere.

point of Viton A are measured where the sample was subjected to heating from −50 °C to 100 °C at heating rate of 10 °C/min under nitrogen atmosphere. Fig. 3 shows DSC curve of Viton A. It is observed that the T_g and softening point are found to be −18 °C and 60 °C respectively. The second DSC curve of Viton A shows a single endothermic peak at 493 °C due to the thermal decomposition of polymer matrices.

DSC curves of PBXs; HT1080, HT2070, HT3060, HT4050, HT5040, HT6030, HT7020 and HT8010 show two endothermic and three exothermic peaks in the DSC curves. The first two endothermic peaks appear at 190 ± 1.5 °C and 278 ± 0.6 °C due to β to δ-HMX phase transformation and melting point respectively. Some of endothermic peaks due to melting point for HT1080, HT2070 and HT3060 samples is not clearly detected in DSC curves, while the first exothermic peak appears within a range of 282 °C −286 °C due to thermal decomposition of HMX and the second exothermic peak appears in a range of 370 °C −380 °C due to thermal decomposition of TATB. The second exothermic peak is not clearly seen in the DSC curves because of overlapping of the multiple DSC curves into in a single curve. The third exothermic peak appears within a range of 484 °C −498 °C due to thermal decomposition of polymer matrices. DSC curves also show that there is no change in thermal decomposition behaviour or a new peak formation for PBXs formulations compared to those individual materials. This confirms that the HMX, TATB and Viton A are compatible with each other. The results obtained by DSC are fully supported to TG thermal data where PBXs exhibit almost the similar thermal decomposition profiles.

The thermal data in terms of T_{onset}, T_{endset}, T_{max} and enthalpy of the decomposition process interpreted from DSC curves are listed in Table 3. It can be seen from Table that the melting point of PBXs is found to very close to the HMX. The T_{max} values are shifted towards a high temperature with increasing the HMX amount, indicating that the thermal stability is slightly decreased with decreasing HMX amount and lower than pure HMX. The enthalpy of

Table 3
The thermal data in terms of T_m, T_{max} and enthalpy of PBXs along with HMX, TATB and Viton A.

Sample	T_m /(°C)	The exo- and endo-thermic peaks for decomposition process					
		1st step		2nd step		3rd step	
		T_{max} /(°C)	ΔH /(J.g^{-1})	T_{max} /(°C)	ΔH /(J.g^{-1})	T_{max} /(°C)	ΔH /(J.g^{-1})
HT1080	–	282.1	142	380.2	772	489.1	102
HT2070	–	282.4	252	378.8	318	484.4	161
HT3060	–	282.9	361	378.2	342	484.9	194
HT4050	278.0	283.0	788	376.3	179	496.1	149
HT5040	278.1	284.8	1050	374.9	80	497.7	169
HT6030	277.8	285.1	1190	374.0	43	489.2	112
HT7020	277.9	285.7	1264	370.1	14	493.0	120
HT8010	278.6	286.1	1345	–	–	494.5	141
HMX	278.0	287.2	1921	–	–	–	–
TATB	–	387.8	1145	–	–	–	–
Viton A	55.9	493.4 (endothermic)	79	–	–	–	–

exothermic decomposition process is found to increase with increasing HMX amount. Table 3 shows that PBXs mass-specific enthalpy of decomposition is comparable with the decomposition enthalpy of pure HMX. The T_{max} value for the second exothermic decomposition process is reduced, while the enthalpy of decomposition process is decreased with increasing the HMX amount. The enthalpy for the third exothermic decomposition process is found in a wide range of 102–194 kJ/mol. The difference in the results obtained are probably due to a broadening of the decomposition peaks and different mass of Viton A in PBXs formulations which is confirmed in TGA profiles during pyrolysis process.

To investigate the effect of HMX amount on T_g, some PBXs samples; HT4050, HT5040, HT6030, HT7020 and HT8010 were subjected to heating from −50 °C to 100 °C at heating rate 10 °C/min under nitrogen atmosphere. DSC curves HT4050, HT5040, HT6030, HT7020 and HT8010 samples are shown in Fig. 4. The thermal data in terms of T_{onset} and T_g are listed in Table 4. It is observed that T_g is found to close with each other as −15.7 ± 0.2 °C which is approximately 3 °C higher than Viton A.

3.3. Kinetics studies

3.3.1. The theoretical background

Solid-state thermal decomposition kinetics can be investigated by TGA or DSC methods [58–60] by measuring a sample property

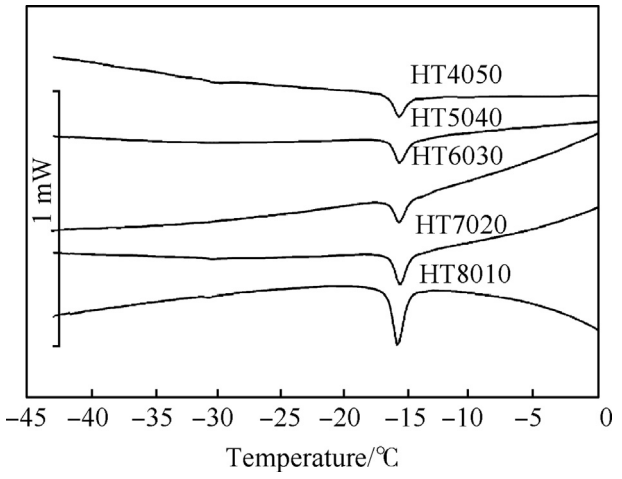

Fig. 4. The T_g and T_{onset} of HT4050, HT5040, HT6030, HT7020 and HT8010 samples at heating rate 10 °C/min under nitrogen atmosphere.

Table 4
The T_{onset} and T_g of HT4050, HT5040, HT6030, HT7020, and HT8010 samples from DSC curves under nitrogen atmosphere.

Sample	T_{onset} /(°C)	T_g /(°C)
HT4050	−16.4	−15.9
HT5040	−16.3	−15.8
HT6030	−16.2	−15.7
HT7020	−16.2	−15.7
HT8010	−16.4	−15.8

as it is heated dynamic or isothermal conditions. Generally, the rate of reaction is described as a linear function of two functions i.e. rate constant (k) and function of the conversion $f(\alpha)$

$$\frac{d\alpha}{dt} = k f(\alpha) \tag{1}$$

where k is a reaction rate constant, α is a extent of conversion, and $f(\alpha)$ is a differential form of the kinetic model, which is a function of α. According to Arrhenius Equation, rate constant which is temperature dependent is described by following Equation (2)

$$k = Ae^{-\frac{E_g}{RT}} \tag{2}$$

where A is a pre-exponential factor, E_a is activation energy, T is absolute temperature and R is the gas constant. For non-isothermal TGA, the conversion (α) at any time T is

$$\alpha = \frac{m_0 - m_T}{m_0 - m_\infty} \tag{3}$$

where, m_o is an initial weight of sample, m_T is a sample weight at temperature T, and m_∞ is a final weight of sample. By substituting of Equation (2) into Equation (1) gives

$$\frac{d\alpha}{dt} = Ae^{-\frac{E_g}{RT}} f(\alpha) \tag{4}$$

For a dynamic TGA in a non-isothermal experimental condition, introducing the heating rate $\phi = dT/dt$ into the Equation (4) gives

$$\frac{d\alpha}{dT} = \frac{A}{\phi} e^{-Ea/RT} f(\alpha) \tag{5}$$

Equations (4) and (5) are fundamental expressions of analytical methods used to investigate kinetic parameters on the basis of the TGA data [61,62]. TG measurements consist of performing the

kinetics analysis which include weight loss curves obtained under dynamic condition.

3.3.2. Flynn-Wall-Ozawa (FWO) method

In general, the activation energies are calculated by model-free methods such as Kissinger-Akahira-Sunose (KAS), Flynn-Wall-Ozawa (FWO) and Friedman methods. The FWO method is a model-free method which is obtained from integral isoconversional method that Flynn, Wall [63] and Ozawa [64] proposed for calculation of activation energy by Doyle's approximation of the temperature integral [65,66].

$$\log(\phi) = \log\frac{A_\alpha E_{a\alpha}}{g(\alpha)R} - 2.315 - 0.457\frac{E_{a\alpha}}{RT_\alpha} \tag{6}$$

where (ϕ) corresponds to the heating rate, T_α is temperature in Kelvin at conversion α, $E_{a\alpha}$ is activation energy in kJ/mol at different conversion α. This is equation of straight line in which $\log(\phi)$ and $1/T_\alpha$, are two variables from which activation energy at given conversion can be obtained from slope of plot $\log(\phi)$ against $1/T_\alpha$.

3.3.3. Kissinger-Akahira-Sunose (KAS) method

This method is also model-free kinetics based on an isoconversional method [67–69] where activation energy is a function of the extent of conversion. KAS method [70] consists of extending the Kissinger's method [71] which is given by Equation (7)

$$\ln\frac{\varphi}{T_\alpha{}^2} = \ln\frac{AR}{E_a\, g(\alpha)} - \frac{E_{a\alpha}}{RT_\alpha} \tag{7}$$

The plot $\ln(\phi/T_a{}^2)$ against $1/T_\alpha$ at a constant value of α should be a straight line and activation energy is calculated from slope of KAS plots.

3.3.4. Calculation of kinetic parameters

The activation energy and pre-exponential factor (A) of thermal decomposition of PBXs are determined by single heating rate measurement and the results are listed in Table 5. The purpose of the present work is to demonstrate the effect of HMX amount on the thermal kinetics. The results show that the activation energy is varied from 524 to 1219 kJ/mol when HMX amount is increased from 10 to 80 percent by wt. It is initially low and then it is started to increase with increasing HMX amount in the first step thermal decomposition. In the second step of decomposition, it is found within a range of 140–153 kJ/mol, while it is observed within a range of 304–366 kJ/mol in the third step thermal decomposition. The activation energy of HMX, TATB and Viton A is also calculated for comparing with PBXs and it is found to be 1295 ± 27.5, 158.5 ± 2.1 and 377.5 ± 3.5 kJ/mol respectively.

For comparison, the activation energy of HT1080 sample is registered close to the literature value of HMX/Viton A formulation [61]. Shi et al. [61] are reported that the activation energy of HMX/Viton A formulation at different heating rates by DSC is 482.7 ± 17.0 kJ/mol using Kissinger method. But the activation energy of the subsequent PBX formulations in our results is increased with increasing the HMX amount. The thermal decomposition process after a certain amount of TATB may be accompanied by fast burning more quickly or deflagration process which can greatly promote the activation energy of PBXs in the first step thermal decomposition.

The activation energy of PBXs based on mixture of HMX and TATB in the second step thermal decomposition is found to be slightly lower than that of pure TATB. The thermal decomposition kinetics of TATB [54] is studied and the activation energy is found to be 42.1 kcal/mol which is close to our results. The activation energy of PBXs in the third step is also observed to be lower than that of Viton A. It is stated that activation energy of Viton A is more varied in the literature. The activation energy of the thermal decomposition derived from TG and decomposition endotherm is 293 and 350 kJ/mol using single heating rate data [72]. Burnham et al. [50] are reported that the activation energy of thermal decomposition of Viton A is 217 kJ/mol using model fitting to correlate reaction data from Freidman isothermal method. Moreover, Papazian [73] is investigated the thermal kinetic of Viton A from single heating experiment and is found the activation energy of 356 kJ/mol.

To evaluate activation energy at different conversion, the

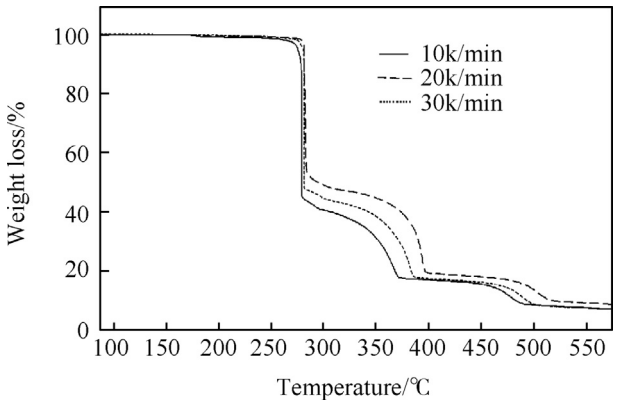

Fig. 5. TG thermograms of HT4050 sample at different heating rates under nitrogen atmosphere.

Table 5
The kinetic parameters for thermal decomposition of PBXs along with HMX, TATB and Viton A.

Sample	Kinetic parameters					
	1st step		2nd step		3rd step	
	E_a/(kJ·mol^{-1})	ln(A) (s^{-1})	E_a/(kJ·mol^{-1})	ln(A) (s^{-1})	E_a/(kJ·mol^{-1})	ln(A) (s^{-1})
HT1080	524.4 ± 22.3	104.4	140.4 ± 2.8	21.2	306.4 ± 8.5	44.7
HT2070	781.8 ± 32.1	166.5	148.7 ± 2.7	22.7	317.9 ± 7.0	46.6
HT3060	1118.3 ± 21.3	242.7	144.6 ± 1.3	22.1	317.3 ± 4.5	46.3
HT4050	1142.3 ± 17.5	244.0	145.7 ± 1.6	22.7	302.8 ± 4.3	43.7
HT5040	1079.4 ± 23.9	242.5	146.6 ± 1.4	23.4	319.4 ± 5.4	46.9
HT6030	1119.6 ± 22.9	243.3	144.2 ± 2.3	23.5	337.2 ± 5.1	49.2
HT7020	1142.3 ± 19.9	244.6	148.9 ± 1.9	23.7	324.6 ± 5.9	47.0
HT8010	1219.7 ± 16.8	261.3	153.5 ± 2.5	24.2	366.8 ± 5.1	56.3
HMX	1295.4 ± 27.5	278.0	–	–	–	–
TATB	–	–	158.5 ± 2.1	25.9	–	–
Viton A	–	–	–	–	377.5 ± 3.5	57.0

thermal decomposition measurement for HT4050 (only one sample) was carried out at 25 °C–600 °C under nitrogen atmosphere. TG thermograms recorded at different heating rates of 10, 20 and 30 °C/min are shown in Fig. 5. TG thermograms show three steps weight loss; 45–55% weight loss occurs in the first step due to thermal decomposition of HMX, while 28–34% weight loss occurs in the second step due to thermal decomposition of TATB. Finally, 9.7–9.8% weight loss attributes to thermal decomposition of Viton A. It can be seen from Fig. 5 that the initial thermal decomposition is shifted towards a high temperature with increasing heating rate.

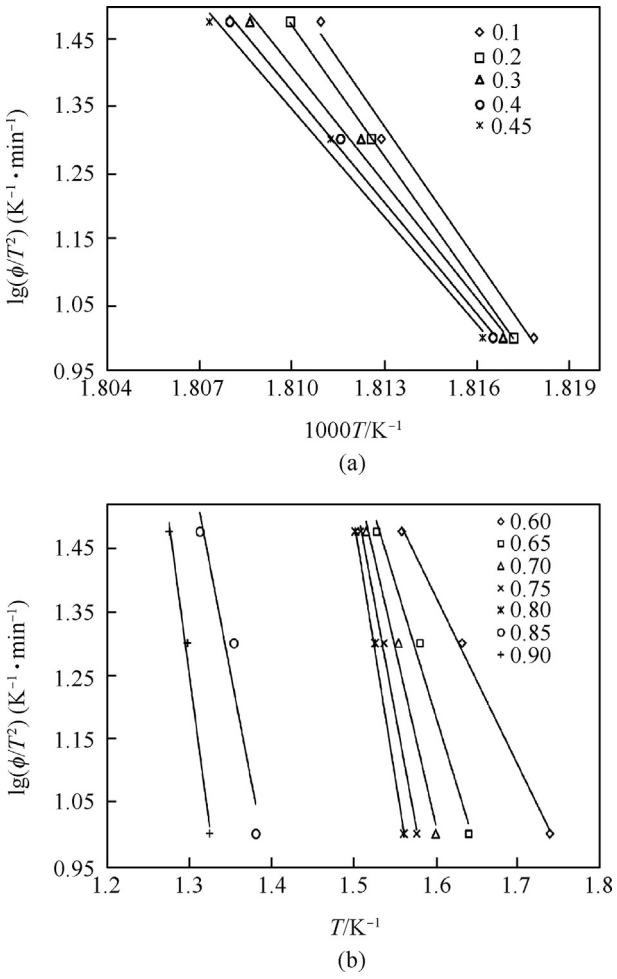

Fig. 6. FWO plots of HT4050 sample at conversion (a) 0.1–0.45, (b) 0.6–0.9.

The activation energy at different conversion (α = 0.1–0.9) is calculated by using FWO Equation (6). Fig. 6 shows FWO plots at different extent of conversion. The activation energy calculated at different conversion and their correlation co-efficient constant are listed Table 6. The activation energies in the first step are found to be 1290.4, 1260.3, 1178.5, 1075.2 and 1035.4 kJ/mol at conversion of 0.1, 0.2, 0.3, 0.4 and 0.45 respectively. The linear correlation co-efficient for each activation energy is high than 0.9909. It is also observed that activation energy is reduced with extent of conversion. The activation energies in the second step are found to 81.9, 108.7, 134.2 and 156.0 kJ/mol at different conversion of 0.65, 0.7, 0.75 and 0.8 respectively, indicating that the activation energy is increased with extent of conversion, while the activation energy in the third step is 186.1 kJ/mol at conversion of 0.9.

According to recommendation of kinetic committee of the International Confederation for Thermal Analysis and Calorimetry (ICTAC) [74], KAS method offers a significant improvement in the accuracy to reliable evaluation of the activation energy by means of TGA compared to FWO method. The activation energy is calculated as a function of conversion by using isoconversional method of KAS Equation (7). The KAS plots at different extent of conversion are shown in Fig. 7. The activation energy obtained from the slope at different extent of conversion (α = 0.1–0.9) are calculated and summarized in Table 7. It can be seen from Table that the activation energy is not same at different extent of conversion indicating multiple reaction mechanisms.

Fig. 8 shows the dependence of the activation energy on extent of conversion. The results show that the activation energy declines about 254.9 kJ/mol when the extent of conversion is changed from 0.1 to 0.45 in the first step, then in the second step the activation energy arises from 71.5 to 145.1 kJ/mol at extent of conversion of 0.65–0.8, and in the third step it arises subsequently from 112.4 to 172.3 kJ/mol as the conversion is changed from 0.85 to 0.9 close to the end of reaction. The mean activation energy calculated by FWO and KAS methods are close and in good agreement to those obtained from single heat rate measurement (1142 ± 17.5 kJ/mol) in the first step decomposition, while in the second and the third steps, there are found difference in the results which can be further improved by calculating the activation energy between 0.8 and 0.85 in the second step as well as 0.9 and 0.95 in the third step where

Table 6
Kinetic parameters for thermal decomposition of HT4050 sample by FWO method.

Conversion (α)	Activation energy and correction coefficient					
	1st step		2nd step		3rd step	
	E_a/(kJ·mol^{-1})	r_a	E_a/(kJ·mol^{-1})	r_a	E_a/(kJ·mol^{-1})	r_a
0.1	1290.4	0.9909	–	–	–	–
0.2	1260.3	0.9999	–	–	–	–
0.3	1117.9	0.9943	–	–	–	–
0.4	1075.2	0.9967	–	–	–	–
0.45	1035.4	0.9941	–	–	–	–
0.6	–	–	51.2	0.9981	–	–
0.65	–	–	81.9	0.9855	–	–
0.7	–	–	108.9	0.9884	–	–
0.75	–	–	134.2	0.9971	–	–
0.8	–	–	156.0	0.9987	–	–
0.85	–	–	–	–	130.0	0.9251
0.9	–	–	–	–	186.1	0.9924
Mean	1168.0 ± 45.4		120.3± 13.8		158.1 ± 19.9	

r_a = correction coefficient for linear regression.

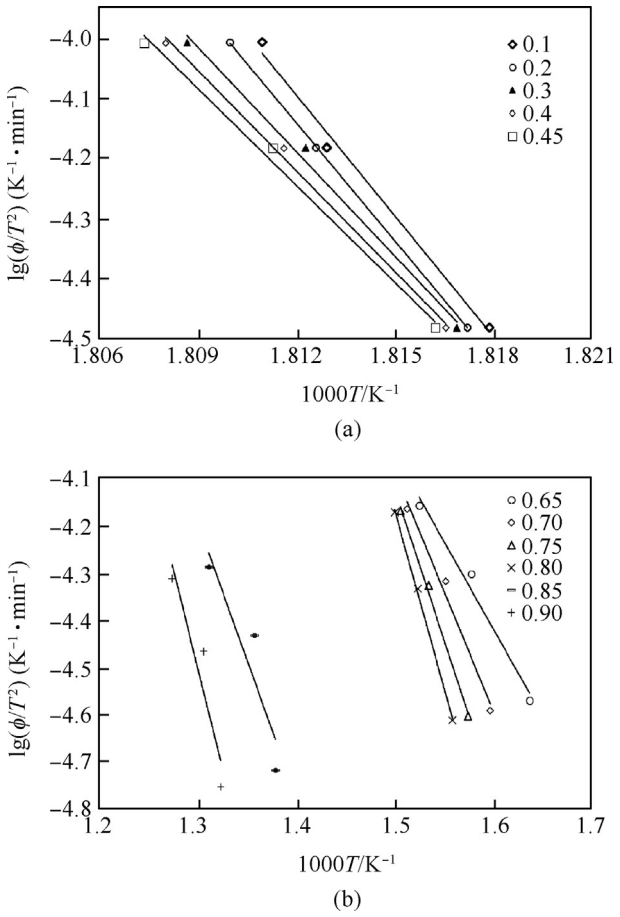

Fig. 7. KAS plots of HT4050 sample at conversion (a) 0.1–0.45, (b) 0.65–0.9.

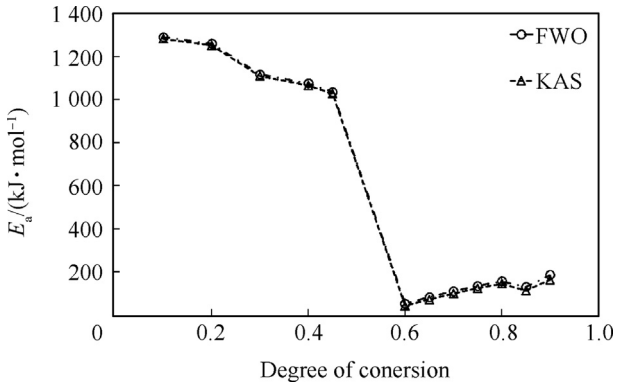

Fig. 8. Dependence of activation energy against extents of conversion.

there may chance to get maximum value of activation energy. The high values of activation energy at low conversion are elucidated due to a high thermal conductivity of TATB which causes the neighbouring HMX molecules to heat up and fast burning more quickly than pure HMX [51]. However, the differences observed in the literature data can also be attributed to the fact that the kinetics for decomposition of HMX depend on the heating rate [75]. Makasher et al. [62] are investigated kinetics of TATB by TGA method and the activation energy is found to 150.58 kJ/mol which is slightly lower than our values. The kinetics by a single heating measurement is meticulously matched with the reliable kinetic evaluations obtained at multiple heating rates in aforementioned FWO and KAS methods.

4. Conclusions

In the present study, the thermal properties such as T_g, T_m and thermal decomposition were investigated for PBXs based on mixture of HMX and TATB with Viton A using STA and DSC. The results indicate that 9–72% weight loss was occurred in the first step due to thermal decomposition of HMX. It was also found that weight loss was increased with increasing HMX amount. TGA indicated that T_{onset} and T_{max} values were slightly increased with increasing HMX amount. These results suggested that the HMX, TATB and Viton A were thermally stable and compatible with each other. The activation energies were ranged from 524 to 1219 kJ/mol, and the natural logarithm of pre-exponential factor were ranged from 104.4 to 261.4 s^{-1} for a single heating rate measurement under non-isothermal condition. The activation energy was significantly increased with increasing the HMX amount in the first step thermal decomposition. The kinetics were also investigated by using FWO and KAS methods. The TGA indicated that the decomposition of HT4050 was occurred in distinct steps at multiple heating rates under non-isothermal condition. The results indicated that activation energies were 1290 to 1050 kJ/mol at conversion of 0.1–0.45, whereas at conversion of 0.65–0.8, the activation energy was ranged from 81.4 to 156.3 kJ/mol, and the

Table 7
Kinetic parameters for thermal decomposition of HT4050 sample by KAS method.

Conversion (α)	Activation energy and correction coefficient					
	1st step		2nd step		3rd step	
	E_a/(kJ·mol^{-1})	r_a	E_a/(kJ·mol^{-1})	r_a	E_a/(kJ·mol^{-1})	r_a
0.1	1282.3	0.9924	–	–	–	–
0.2	1251.9	0.9989	–	–	–	–
0.3	1109.2	0.9932	–	–	–	–
0.4	1065.5	0.9960	–	–	–	–
0.45	1027.4	0.9923	–	–	–	–
0.6	–	–	41.1	0.9981	–	–
0.65	–	–	71.5	0.9855	–	–
0.7	–	–	98.2	0.9884	–	–
0.75	–	–	123.4	0.9971	–	–
0.8	–	–	145.1	0.9987	–	–
0.85	–	–	–	–	112.4	0.9251
0.9	–	–	–	–	172.3	0.9924
Mean	1147.3 ± 45.5		109.6 ± 13.8		142.4± 21.1	

third step decomposition the activation energy was attributed to 130 and 186.1 kJ/mol at conversion of 0.85 and 0.9 respectively by FWO method. The activation energy calculated by both FWO and KAS methods was close to each other. The mean activation energy was also a good agreement with a single heating rate measurement in the first step decomposition.

Acknowledgements

The authors would like to express their sincere thanks to DRDO (TBR-1251) for funding and awarding the Project. The authors are expressed their sincere thanks to Sh. C. Sarkar, Sh. N. Mukherjee, Dr. P. K. Soni and Dr. Manjit Singh, Distinguished Scientist/Director TBRL for their motivation, guidance and constant help provided during the execution of this work.

References

[1] Mattos EC, Moreira ED, Diniz MF, Dutra RCL, Silva G, Iha K, Teipel U. Characterization of polymer-coated RDX and HMX particles. Propellants Explos Pyrotech 2008;33(1):44–50.
[2] Yan QL, Zeman S, Elbeih A. Recent advances in thermal analysis and stability evaluation of insensitive plastic bonded explosives (PBXs). Thermochim Acta 2012;537:1–12.
[3] Agrawal JP. 2005. Some new high energy materials and their formulations for specialized applications. Propellants Explos Pyrotech 2005;30(5):316–28.
[4] Boddu VM, Viswanath DS, Ghosh TK, Damavarapu R. 2,4,6-Triamino-1,3,5-trinitrobenzene (TATB) and TATB-based formulations-A Review. J Hazard Mater 2010;181(1):1–8.
[5] Schaffer CL. Compositional analysis of PBX 9503-A TATB/HMX/Kel-F800 formulation. Report MHSMP-81–55, DE 82006183. USA: Department of Energy; 1981.
[6] Provatas A. Formulation and performance studies of polymer bonded explosives (PBX) containing energetic binder systems. Part 1, Report DSTO-TR-1397. Edinburgh, Australia: Weapons Systems Division, Systems Sciences Laboratory; 2003.
[7] Nandi AK, Ghosh M, Sutar V, Pandey RK. Surface coating of cyclotetramethylenetetranitramine (HMX) crystals with the insensitive high explosive1,3,5-triamino-2,4,6-trinitrobenzene (TATB). Central Eur J Energetic Mater 2002;9(2):119–30.
[8] Kaur J, Arya VP, Kaur G, Lata P. Evaluation of the thermo-mechanical and explosive properties of bimodal and hybrid polymer bonded explosive (PBX) compositions based on HNS and HMX. Central Eur J Energetic Mater 2013;10(3):371–91.
[9] Guo H, Luo J-R, Shi P-A, Xu J-G. Research on the fracture behavior of PBX under static tension. Def Technol 2014;10:154–60.
[10] Tian Y, Xu R, Zhou Y, Nie F. Study on formulation of CL-20. In Proceedings of the 4th International Autumn Seminar on Propellants, Explosives and Pyrotechnics, Shaoxing, China 2001 pp. 43–47.
[11] An C, Wang J, Xu W. Preparation and properties of HMX coated with a composite of TNT/energetic material. Propel Explos Pyrotech 2010;35:365–72.
[12] Nair UR, Asthana SN, Rao AS, Gandhe BR. Advances in high energy materials. Def Sci J 2010;60(2):137–51.
[13] Turker L. Thermobaric and enhanced blast explosives (TBX and EBX). Def Technol 2016;12(6):423–35.
[14] Elbeih A, Husarova A, Zeman S. Path to ε-HNI W with reduced impact sensitivity. Cent Eur J Energ Mater 2011;8(3):173–82.
[15] Agrawal JP. High energy materials, propellants, explosives and pyrotechnics. Wiley- VCH; 2010. p. 69–150. Chapter 2.
[16] Sorescu DC, Boatz JA, Thompson DL. Classical and quantum mechanical studies of crystalline FOX-7 (1, 1 diammino- 2, 2- dinitroethylene). J Phys Chem 2001;105(20):5010–21.
[17] Steele RD, Stretz LA, Taylor GW, Rivera T. Effects of Binder Concentration on the Properties of Plastic Bonded Explosives. Proceedings of the Ninth Symposium (International) on Detonation, Office of the Chief of Naval Research OCNR 113291–7, Portland, OR 1989 August 28, pp. 1014–1018.
[18] Talwar MB, Agrawal AP, Anniyappan M, Gore GM, Asthana SN, Venugopalan S. Method for preparation of fine TATB (2–5 μm) and its evaluation in plastic bonded explosive (PBX) formulations. J Hazard Mater 2006;137:1848–52.
[19] Boddu VM, Viswanath DS, Ghosh TK, Damavarapu R. 2,4,6-Triamino-1,3,5-trinitrobenzene (TATB) and TATB-based formulations-a review. J Hazard Mater 2010;18:1–8.
[20] Dobratz BM. The insensitive high explosive Triaminotrinitrobenzene (TATB): development and characterization-1888 to 1994. report LA-13024H. Los Alamos: National Laboratory; August 1994.
[21] Willey TM, DePiero SC, Hoffman DM. A Comparison of New TATBs, FK-800 binder and LX-17-like PBXs to Legacy Materials, 1st Korean International Symposium on High Energy Materials Incheon, South Korea October 6-9, 2009.
[22] Gibbs TR, Popolato A. LASL high explosive property data. California, Berkeley: University of California Press; 1980. p. 1–30.
[23] Maienschein JL, Garcia F. Thermal expansion of TATB based explosives from 300 K to 566 K. Thermochim Acta 2002;384:71.
[24] Ninan KN, Krishnan K, Rajeev R, Viswanathan G. Thermo analytical investigations on the effect of atmospheric oxygen on HTPB resin. Propel Explos Pyrotech 1996;21:199.
[25] Voreck W, James B, John E, Hooshang R. Shaped charge for a perforating gun having a main body of explosive including TATB and a sensitive primer. United States Patent 5597974; 1997.
[26] Voreck W, James B, John E, Hooshang R. Shaped charge containing triaminotrinitrobenzene (TATB), European Patent, EP-0794163 1997.
[27] Cooper PW. Explosive engineering. New York: Wiley-VCH; 1996.
[28] Aggarwal P, Singh V, Singh A, Scherer UW, Singh T, Singla ML, et al. Physicochemical transformation in swift heavy ion modified poly(-etheneterephthalate). Radiat Phys Chem 2012;81:284.
[29] Qiu L, Xiao H. Molecular dynamics study of binding energies, mechanical properties, and detonation performances of bicyclo-HMX-based PBXs. J Hazard Mater 2009;164:329–36.
[30] Xiao JJ, Fang GY, Ji GF, Xiao HM. Simulation investigation in the binding energy and mechanical properties of HMX-based plastic- bonded explosives (PBXs). Chin Sci Bull 2005;50(1):21–26.9.
[31] Xiao JJ, Huang YC, Hu YJ, Xiao HM. Molecular dynamics simulation of mechanical properties of TATB/Flourine-polymer PBXs along different surfaces. Sci China Ser B-Chem 2005;48:504–10.
[32] Manaa MR, Fried LE, Melius CF, Elstner M, Frauenheim T. Decomposition of HMX at extreme conditions: a molecular dynamics simulation. J Phys Chem A 2002;106:9024–9.
[33] Ma XF, Xiao JJ, Huang H, Ju XH, Li JS, Xiao HM. Simulative calculation on mechanical property, binding energy and detonation property of TATB/fluorine-polymer PBX. Chin J Chem 2006;24:473–7.
[34] Song XL, Wang Y, An CW, Guo XD. Dependence of particle morphology and size on the mechanical sensitivity and thermal stability of octahydro-1,3,5,7-tetranitro-1,3,5,7-tetrazocine. J Hazard Mater 2008;159(2–3):222–9.
[35] Tarver CM. Modeling detonation experiments on triaminotrinitrobenzene (TATB)-based explosives LX-17, PBX 9502, and Ultrafine TATB. J Energ Mater 2012;30(3):220–51.
[36] Elbeih A, Zeman S, Jungova M, Akstein Z. Effect of different polymeric matrices on the sensitivity and performance of interesting cyclic nitramines. Cent Eur J Energ Mater 2012;9(2):131–8.
[37] Elbeih A, Pachman J, Zeman S, Vávra P, Trzciński WA, Akštein Z. Detonation characteristics of plastic explosives based on attractive nitramines with polyisobutylene and poly(methyl methacrylate) binders. J Energ Mater 2012;30(4):358–71.
[38] Lee JS, Hsu CK, Chang CLA. Study on the thermal decomposition behaviors of PETN, RDX, HNS and HMX. Thermochim Acta 2002;392–393:173–6.
[39] Fu XL, Fan XZ, Wang BZ. Thermal behavior, decomposition mechanism and thermal safety of 5,7-diamino-4,6-dinitrobenzenfuroxan (CL-14). J Therm Anal Calorim 2016;124:993.
[40] Yan Q-L, Zeman S, Sánchez Jiménez PE, Zhao F-Q, Pérez-Maqueda LA, Málek J. The effect of polymer matrices on the thermal hazard properties of RDX-based PBXs by using model-free and combined kinetic analysis. J Hazard Mater 2014;271:185–95.
[41] Singh G, Felix SP, Soni P. Studies on energetic compounds Part 31: thermolysis and kinetics of RDX and some of its plastic bonded explosives. Thermochim Acta 2005;426:131–9.
[42] Singh G, Felix SP, Soni P. Studies on energetic compounds part 28: thermolysis of HMX and its plastic bonded explosives containing Estane. Thermochim Acta 2003;399:153–65.
[43] Zeman S, Elbeih A, Akstein Z. Preliminary study on several plastic bonded explosives based on cyclic nitramines. Chin J Energ Mater 2011;19(1):8–12.
[44] Yan Q-L, Zeman S, Zhang X-H, Málek J, Xie W-X. The mechanisms for desensitization effect of synthetic polymers on BCHMX: physical models and decomposition pathways. J Hazard Mater 2015;294:145–57.
[45] Yan Q-L, Zeman S, Elbeih A. Thermal behavior and decomposition kinetics of Viton A bonded explosives containing attractive cyclic nitramines. Thermochim Acta 2013;562(20):56–64.
[46] Yan Q-L, Zeman S, Zhao F-Q, Elbeih A. Non-isothermal analysis of C4 bonded explosives containing different cyclic nitramines. Thermochem Acta 2013;556:6–12.
[47] Yan Q-L, Zeman S, Zhang T-L, Elbeih A. Non-isothermal decomposition behavior of Fluorel bonded explosives containing attractive cyclic nitramines. Thermochim Acta 2013;574:10–8.
[48] Yan Q-L, Zeman S, Zhang T-L, Elbeih A, Akstein Z. The Influence of the Semtex matrix on the thermal behavior and decomposition kinetics of cyclic nitramines. Central Eur J Energetic Mater 2013;10(4):509–28.
[49] Clements BE, Mas EM. A theory for plastic-bonded materials with a bimodal size distribution of filler particles. Modell Simul Mater Sci Eng 2004;12:407–21.
[50] Burnham AK, Weese RK. Kinetics of thermal degradation of explosive binders Viton A, Estane and Kel-F. Thermochim Acta 2005;426:85–92.
[51] Craig M, Tarver J, Koerner G. Effects of endothermic binders on times to explosion of HMX- and TATB-based plastic bonded explosives. J Energetic Mater 2007;26(1):1–28.

[52] McGuire RR, Tarver CM. Chemical Decomposition Models for the Thermal Explosion of Confined HMX, TATB, RDX, and TNT Explosives. Proceedings of the Seventh Symposium (International) on Detonation, Naval Surface Weapons Center NSWC MP 82–334, Annapolis MD, 1981; 16, pp. 56–65.
[53] Lin CP, Chang YM, Tseng JM, Shu C-M. Comparisons of nth-order kinetic algorithms and kinetic model simulation on HMX by DSC tests. J Therm Anal Calorim 2010;100:607.
[54] Tsyshevsky RV, Sharia O, Kuklja MM. Molecular theory of detonation initiation: insight from first principles modelling of the decomposition mechanisms of organic nitro energetic materials. Molecules 2016;21:236.
[55] Singh A, Kumar M, Soni PK, Singh M, Srivastava A. Mechanical and explosive properties of plastic bonded explosives based on mixture of HMX and TATB. Def Sci J 2013;63(6):622–9.
[56] Ger MD, Hwu WH, Huang CC. A study on the thermal decomposition of mixtures containing an energetic binder and a nitramine. Thermochim Acta 1993;224:127–40.
[57] Chakraborty D, Muller RP, Dasgupta S, Goddard WA. Mechanism for unimolecular decomposition of HMX (1,3,5,7-tetranitro-1, 3, 5, 7-tetrazocine), an ab initio study. J Phys Chem A 2001;105(8):1302–14.
[58] Brown ME. Introduction to thermal analysis: techniques and applications. London: Chapman and Hall; 1988. p. 127–51.
[59] Brown ME. Introduction to thermal analysis: techniques and applications. 2nd ed. Amsterdam: Kluwer; 2001. Chapter 10.
[60] Bianchi O, Martins J, De N, Fiorio R, Oliveira RVB, Canto LB. Changes in activation energy and kinetic mechanism during EVA crosslinking. Polym Test 2011;30:616–24.
[61] Shi X, Wang J, Li X, An C, Wang J, Ji W. Preparation and properties of 1,3,5,7,tetranitro- 1,3,5,7 tetraazocane based nanocomposite. Def Sci J 2015;65(2):131–4.
[62] Makashir PS, Kuriam EM. Spectroscopic and thermal studies of the decomposition of 1,3,5 triammino 2,4,6ntrinitrobenzene (TATB). J Anal Calorim 1996;46(1):225–36.
[63] Flynn JH, Wall LA. General treatment of the thermogravimetry of polymers. J Res Natl Bur Std, A Phys Chem 1966;70:487–523.
[64] Ozawa T. A new method of analyzing thermogravimetricdata. Bull Chem Soc Jpn 1965;38:1881–6.
[65] Zoglio MA, Windheuser JJ, Vatti R, Maulding HV, Kornblum Jr SS, Jacobs AL, et al. Pharm Sci Linear nonisothermal Stab Stud 1968;57:2080–5.
[66] Doyle CD. Estimating isothermal life from thermogravimetric data. J Appl Polym Sci 1962;6. 639–632.
[67] Vyazovkin S, Wight CA. Model-free and model-fitting approaches to kinetic analysis of isothermal and nonisothermal data. Thermochim Acta 1999;340:53–68.
[68] Vyazovkin SV, Goryachko VI, Lesnikovich AI. An approach to the solution of the inverse kinetic problem in the case of complex processes. Part III. Parallel independent reactions. Thermochim Acta 1992;197:41–51.
[69] Vyazovkin S. Conversion dependence of activation energy for model DSC curves of consecutive reactions. Thermochim Acta 1994;236:1–13.
[70] Poletto M, Zattera AJ, Santana MC. Thermal decomposition of wood: kinetics and degradation mechanisms. Bioresour Technol 2012;126:7–12.
[71] Kissinger HE. Reaction kinetics in differential thermal analysis. Anal Chem 1957;29:1702–6.
[72] Cuccuru P, Manfredini S, Argiero L. La Chim e Indus 1973;55:6.
[73] Papazian HA. Prediction of polymer degradation kinetics at moderate temperature from TGA measurements. J Appl Polym Sci 1972;16:2503.
[74] Vyazovkina S, Burnham AK, Criado JM, Pérez-Maqueda LA, Popescu C, Sbirrazzuoli N. ICTAC Kinetics Committee recommendations for performing kinetic computations on thermal analysis data. Thermochim Acta 2011;520:1–19.
[75] Pinheiro GFM, Lourenço VL, Iha K. Influence of the heating rate in the thermal decomposition of HMX. J Therm Analysis Calorim 2002;67:445–52.